

## Wideband Microstrip Filters

B. A. Belyaev<sup>a, b\*</sup>, S. A. Khodenkov<sup>a</sup>, I. V. Govorun<sup>a, c</sup>, and A. M. Serzhantov<sup>a, b</sup>

<sup>a</sup> Siberian State University of Science and Technology, Krasnoyarsk, 660037 Russia

<sup>b</sup> Siberian Federal University, Krasnoyarsk, 660041 Russia

<sup>c</sup> Kirensky Institute of Physics, Krasnoyarsk Scientific Center, Siberian Branch,  
Russian Academy of Sciences, Krasnoyarsk, 660036 Russia

\*e-mail: belyaev@iph.krasn.ru

Received October 13, 2020; revised December 15, 2020; accepted December 24, 2020

**Abstract**—New microstrip designs of bandpass filters have been developed on the basis of a low-pass filter with some or all of the sections of the high-impedance microstrip lines connected to a screen by stubs. The filters exhibit the high frequency selectivity and their fractional bandwidth falls within the range of 30–150%. An experimental sample filter with a passband center frequency of 2 GHz and a fractional bandwidth of 70% formed on a 1-mm-thick alumina substrate has a substrate area of  $46 \times 21$  mm. It is shown that the measured frequency responses of the filter are in good agreement with those calculated using the numerical electrodynamic analysis of its 3D model.

**Keywords:** bandpass filter, microstrip resonator, dielectric substrate, frequency response

**DOI:** 10.1134/S1063785021040039

Enhancing the data transmission rate is one of the most important tasks in digital radio communication systems, which is frequently solved via broadening the working band. Such systems require highly selective ultrawideband bandpass filters, which have been intensively designed in recent years. These filters are known to be easily implemented by cascading a low-pass filter (LPF) with a high-pass filter [1, 2]. However, great interest is presented are simpler and more manufacturable microstrip coupled resonators filter designs, in which the screen metallization is partially removed to enhance the coupling between resonators [3, 4] or triple-mode resonators are used [5]. In this case, for filters with a fractional bandwidth  $\Delta f/f_0$  of broader than 100%, microstrip designs based on irregular quarter-wave resonators coupled either conductively [6, 7] or inductively [8] are better applicable.

We studied a new design of an ultrawideband bandpass filter based on a seventh-order microstrip LPF, whose conductor topology and frequency response are shown in Fig. 1. The characteristic impedance of the filter input and output ports is  $50 \Omega$ . The 1-mm-thick LPF alumina substrate with a permittivity of  $\epsilon = 9.8$  at a filter cutoff frequency of 2.5 GHz has a relatively small ( $40 \times 16$  mm) area due to an irregular conductor folded in two. The dimensions of regular strip conductor sections of the structure are indicated in millimeters in Fig. 1. Folding of the LPF conductor not only reduces the substrate length, but also increases the slope of the frequency response [9] due to the occur-

rence of an additional electromagnetic coupling between nonadjacent resonators [10].

An LPF turns to a bandpass filter if some or all narrow sections of its irregular conductor are connected to the screen by stubs. In this case, each stub not only works as a parallel inductance, as in high-pass filters, but is also a mutual inductance of adjacent resonators, the value of which determines their coupling. Figure 2 shows frequency responses of four filters, in the first of which only two sections designated by Roman numeral I on the LPF conductor topology (Fig. 1) are closed to the screen. In the second filter, four sections designated by numerals I and II are closed; in the third one, six (I, II, and III) are closed; and, in the fourth filter, all the seven narrow sections are closed. The filters were tuned by selecting the conductor width at the stubs and slightly displacing the point of their connection relative to the middle of the narrow conductors so that the maxima of return loss in the filter passband were about  $-20$  dB. For clarity, Fig. 2 shows the frequency dependence of the return loss for only the fourth filter.

For all four filter designs, Table 1 gives passband center frequency  $f_0$ , fractional bandwidth  $\Delta f/f_0$  measured at a level of  $-3$  dB of the minimum loss, which was no higher than 0.4 dB, and coefficients of the low-frequency slope  $k_l$  and the high-frequency slope  $k_h$  of the frequency response calculated using the formulas [11]

$$k_l = \frac{\Delta f / 2}{\Delta f_{30}^l - \Delta f / 2}, \quad k_h = \frac{\Delta f / 2}{\Delta f_{30}^h - \Delta f / 2}, \quad (1)$$

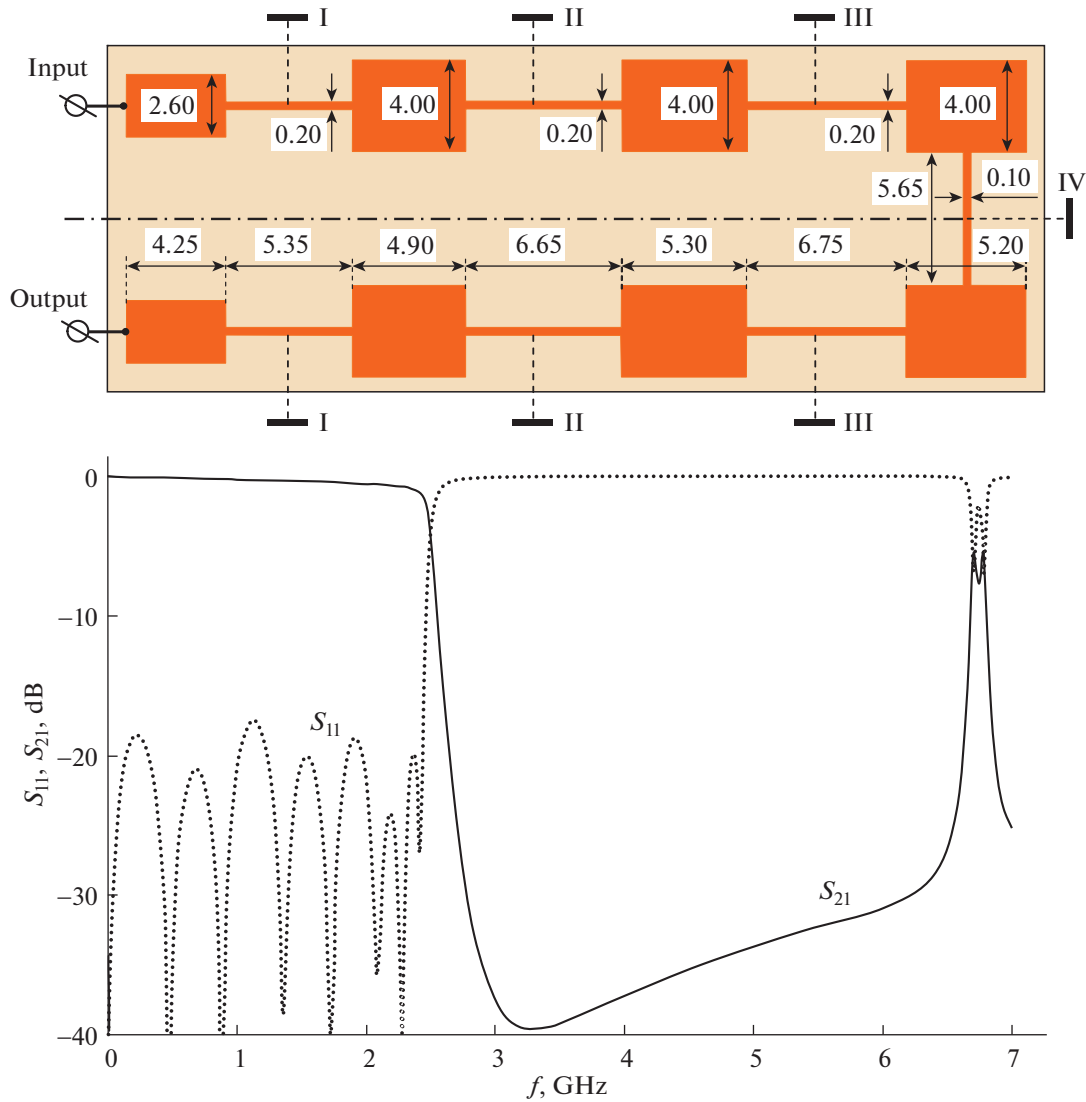


**Fig. 1.** Topology of a strip conductor of the low-pass filter (the dimensions of regular sections of the strip conductor of the structure are given in mm) and frequency dependences of its insertion loss (solid line) and return loss (dashed line).

where  $\Delta f_{30}^l$  and  $\Delta f_{30}^h$  are the frequency bands measured from the center frequency to the low- or high-frequency slope of the frequency response at a level of  $-30$  dB.

It can be seen from Table 1 that the bandpass center frequency for the first filter design is  $f_0 = 1.4$  GHz and uniformly increases by 100 MHz for each next design. The fractional bandwidth  $\Delta f/f_0$  uniformly decreases from 150% for the first design to 90% for the fourth one. In addition, Table 1 shows that the steepness of the high-frequency slope of the frequency response for all the filters is higher than that of the low-frequency slope; however, as the fractional bandwidth decreases, the steepness of the slopes is gradually leveled and the frequency response becomes almost symmetric. Importantly, in all the investigated designs, the bandwidth of the devices can be smoothly tuned within

narrow limits by changing the stub length. However, in the fourth filter design, the fractional bandwidth can be reduced by a factor of 3 (from 90 to 30%) with simultaneous shortening of the all seven closing stubs.

The operation of the developed ultrawideband filters was experimentally tested on the fourth of the investigated designs, in which all the seven stubs are closed to the screen. A 1-mm-thick alumina plate was used as a substrate of the experimental device. For certainty, the center frequency of the filter passband and its fractional bandwidth were specified to be  $f_0 = 2$  GHz and  $\Delta f/f_0 = 70\%$ . Parametric synthesis of the structure was carried out using the numerical electrodynamic analysis of its 3D model in the CST Studio Suite software package so that all maxima of the return loss in the passband were at a level of  $-20$  dB.

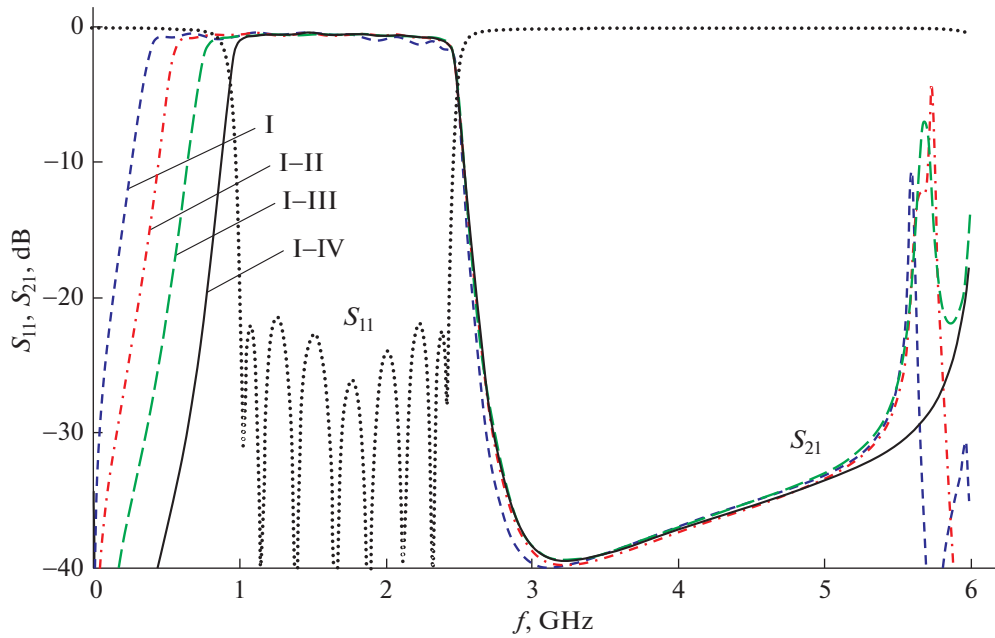


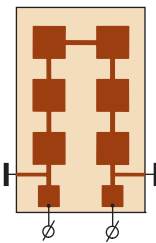
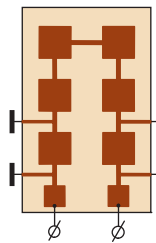
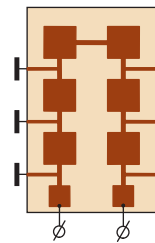
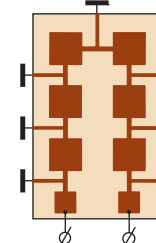
Fig. 2. Frequency response of the bandpass filters with some or all narrow sections of an irregular LPF conductor closed to the screen.

The dimensions (in millimeters) of the conductor topology of the synthesized filter design are shown in Fig. 3a and the calculated frequency response of insertion loss is shown in Fig. 3b (solid line). It should be noted that, at the stub ends of the investigated design, there are square pads  $1 \times 1$  mm in size for increasing the strength of conductors during soldering and at the ends of the ports, which are brought out to opposite substrate sides for convenience of connecting the filter. Note also that, between the wide sections of conductors of the input and output resonators in the filter, a rectangular conductor of the same length was added, which has 0.3-mm gaps with them (Fig. 3a). The conductor ensures additional coupling between these res-

onators, due to which a damping pole is formed near the high-frequency slope of the frequency response [9, 10], which significantly increases the slope (Fig. 3b).

The design parameters (Fig. 3a) yielded by the filter synthesis according to the specified passband parameters were used to fabricate the conductor topology on a metallized alumina substrate  $46 \times 21$  mm in size. The obtained microstrip structure was soldered to the bottom of a metal case with its lower base (screen), and, then, the contact pads of the stubs were soldered to the side walls of the case. A photograph of the fabricated experimental sample is shown in the inset to Fig. 3b. Frequency dependences of the

Table 1. Parameters of the frequency response for the four bandpass filter designs

Parameter	Filter design			
				
$f_0$ , GHz	1.4	1.5	1.6	1.7
$\Delta f/f_0$ , %	150	130	110	90
$k_l$	3.44	2.57	2.48	2.36
$k_h$	4.63	3.61	3.24	2.85

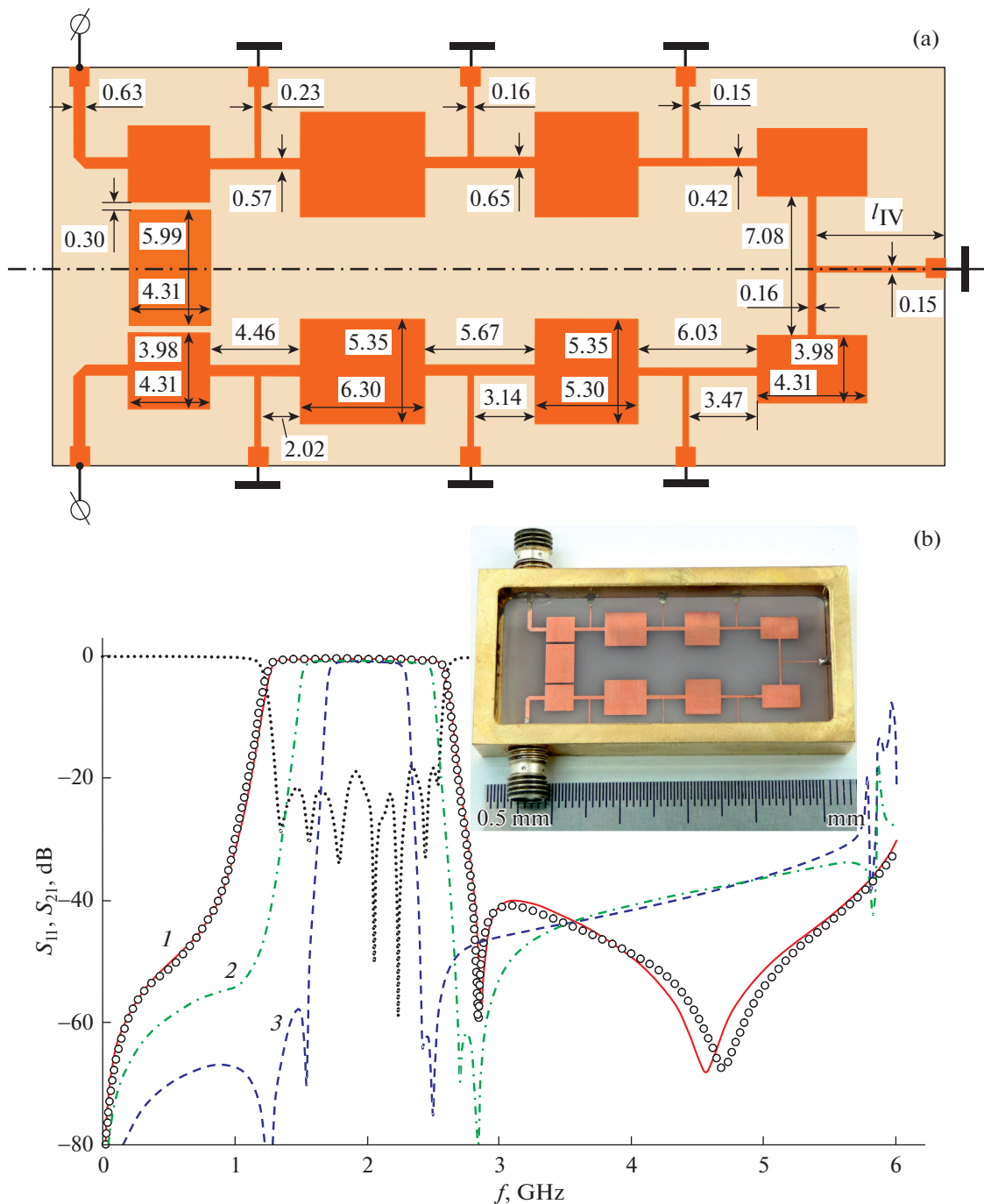


**Fig. 3.** (a) Topology of conductors with dimensions (mm) of regular sections of the synthesized filter. (b) Lines show frequency dependences of insertion loss of the filters with  $\Delta f/f_0 = (1)$  70, (2) 50, and (3) 30%. Points show the measured frequency responses of the experimental sample filter with  $\Delta f/f_0 = 70\%$ . The inset shows its photograph.

insertion loss  $S_{21}$  and return loss  $S_{11}$  measured on an R&S ZVA-40 vector network analyzer are shown in Fig. 3b by open circles and dotted lines, respectively. Note not only the good agreement between the calculated and measured frequency characteristics of the filter, but also the same minimum loss  $L_{\min} = 0.4$  dB in the passband of the device in theory and experiment.

As was mentioned above, the simultaneous shortening of all stub lengths in the investigated design leads to a decrease in the bandwidth. Figure 3b shows the frequency responses of the filters with a fractional bandwidth of 50% (line 2) and 30% (line 3). Note that, in the designs of these filters, due to the small stub length (Table 2), it was necessary to move the sections of the narrow conductors connected to the screen by

**Table 2.** Parameters of the frequency response for the filters with all stubs of length  $l_{\text{I}}-l_{\text{IV}}$  closed to the screen tuned to a passband center frequency of 2 GHz

$l_{\text{I-III}}$ , mm	$l_{\text{IV}}$ , mm	$\Delta f/f_0$ , %	$L_{\text{min}}$ , dB	$k_l$	$k_h$
4.71	6.65	70	0.4	2.85	4.00
1.78	2.80	50	0.7	3.06	4.14
1.06	1.70	30	0.9	3.22	4.46

stubs from the centers to the edges of wide conductors (Fig. 3a). In this case, the distance from the edges of wide conductors to the substrate edges is always larger than 1 mm, i.e., than its thickness. To compare the characteristics objectively, the filters were tuned by the parametric synthesis to the same center frequency  $f_0 = 2$  GHz, also in the CST Studio Suite software package.

For the filters the frequency responses of which are shown in Fig. 3b, Table 2 gives not only the stub lengths, but also the main parameters of the frequency response. As expected, the level of minimum loss  $L_{\text{min}}$  in the passband monotonically increases as its width decreases. Steepness  $k_h$  of the high-frequency slope of the frequency response for all the filters is significantly larger than  $k_l$  due to the damping pole formed owing to a specially induced coupling between the edge resonators. However, with a decrease in the filter bandwidth, the gaps between wide conductors of the internal resonators in the microstrip structure decrease, additional connections are formed between nonadjacent resonators, and, as a result, new poles appear in the filter frequency response, which increase the low-frequency slope.

Thus, new designs were developed for the bandpass filters based on a microstrip LPF consisting of alternating sections of wide (low-impedance) and narrow (high-impedance) conductors, in which some or all high-impedance conductors are connected to the screen by stubs. The study of these structures showed the possibility of using them to implement filters with fractional bandwidths from 30 to 150%, which are characterized by simplicity and high manufacturability. Simultaneously, the devices have a relatively high frequency selectivity due to the simplicity of forming additional connections between nonadjacent resonators in the developed designs, which results in the appearance of damping poles in the frequency dependences of insertion loss significantly increasing the slope of the frequency response. The measured characteristics of the experimental filter with a relative bandwidth of 70% on alumina substrate showed good agreement with the calculated characteristics obtained by the electrodynamic analysis of a 3D model of the structure. These facts are indicative of the potential of the proposed designs for creating ultrawideband filters, which are in great demand, e.g., in high-speed radio communication systems.

## FUNDING

This study was supported by the Ministry of Science and Higher Education of the Russian Federation, state assignment FEFE-2020-0013.

## CONFLICT OF INTEREST

The authors declare that they have no conflict of interest.

## REFERENCES

1. C.-L. Hsu, F.-C. Hsu, and J.-T. Kuo, in *Proceedings of the IEEE MTT-S International Microwave Symposium* (Long Beach, CA, 2005), p. 679. <https://doi.org/10.1109/MWSYM.2005.1516698>
2. B. A. Belyaev, A. M. Serzhantov, An. A. Leksikov, Ya. F. Bal'va, and E. O. Grushevskii, *Tech. Phys. Lett.* **46**, 787 (2020). <https://doi.org/10.1134/S1063785020080179>
3. Ya. A. Kolmakov and I. B. Vendik, in *Proceedings of the 35th European Microwave Conference 2005* (Paris, 2005), Vol. 1, p. 21. <https://doi.org/10.1109/EUMC.2005.1608783>
4. S. Shang, B. Wei, B. Cao, X. Guo, X. Wang, and L. Ji-ang, *IEEE Trans. Appl. Supercond.* **29**, 1500105 (2019). <https://doi.org/10.1109/TASC.2018.2880331>
5. B. A. Belyaev, S. A. Khodenkov, An. A. Leksikov, and V. F. Shabanov, *Dokl. Phys.* **62**, 289 (2017). <https://doi.org/10.7868/S0869565217180062>
6. R. Zhang, S. Luo, and L. Zhu, *IEEE Trans. Microwave Theory Tech.* **65**, 815 (2017). <https://doi.org/10.1109/TMTT.2016.2636825>
7. Y. Zhu, K. Song, and Y. Fan, *IEEE Access* **7**, 117219 (2019). <https://doi.org/10.1109/ACCESS.2019.2928342>
8. K.-D. Xu, D. Li, and Y. Liu, *IEEE Microwave Wireless Comp. Lett.* **29**, 107 (2019). <https://doi.org/10.1109/LMWC.2019.2891203>
9. B. A. Belyaev, S. A. Khodenkov, and V. F. Shabanov, *Dokl. Phys.* **64**, 85 (2019). <https://doi.org/10.31857/S0869-5652485127-32>
10. B. A. Belyaev, A. M. Serzhantov, Y. F. Bal'va, V. V. Tyurnev, A. A. Leksikov, and R. G. Galeev, *Microwave Opt. Technol. Lett.* **56**, 2021 (2014). <https://doi.org/10.1002/mop>
11. B. A. Belyaev, A. A. Leksikov, and V. V. Tyurnev, *J. Commun. Technol. Electron.* **49**, 1228 (2004).

*Translated by E. Bondareva*